Received: 7 August 2018 | Revised: 9 October 2018 | Accepted: 20 November 2018

DOI: 10.1111/pce.13488

ORIGINAL ARTICLE

WILEY Plant, Cell & Environment

# Carbon balance and source-sink metabolic changes in winter wheat exposed to high night-time temperature

Somayanda M. Impa[1] | V.S. John Sunoj[1] | Inga Krassovskaya[2] | Raju Bheemanahalli[1] | Toshihiro Obata[2] | S.V. Krishna Jagadish[1]

[1] Department of Agronomy, Throckmorton Plant Sciences Center, Kansas State University, Manhattan, Kansas, USA

[2] Department of Biochemistry and Center for Plant Science Innovation, University of Nebraska Lincoln, Lincoln, Nebraska

**Correspondence**
S. V. Krishna Jagadish, Department of Agronomy, 2004 Throckmorton Plant Sciences Center, 1712 Claflin Road, Manhattan, KS 66506-5501, USA.
Email: kjagadish@ksu.edu

**Funding information**
National Science Foundation of USA, Grant/Award Number: 1736192

## Abstract

Carbon loss under high night-time temperature (HNT) leads to significant reduction in wheat yield. Growth chamber studies were carried out using six winter wheat genotypes, to unravel postheading HNT (23°C)–induced alterations in carbon balance, source-sink metabolic changes, yield, and yield-related traits compared with control (15°C) conditions. Four of the six tested genotypes recorded a significant increase in night respiration after 4 days of HNT exposure, with all the cultivars regulating carbon loss and demonstrating different degree of acclimation to extended HNT exposure. Metabolite profiling indicated carbohydrate metabolism in spikes and activation of the TriCarboxylic Acid (TCA) cycle in leaves as important pathways operating under HNT exposure. A significant increase in sugars, sugar-alcohols, and phosphate in spikes of the tolerant genotype (Tascosa) indicated osmolytes and membrane protective mechanisms acting against HNT damage. Enhanced night respiration under HNT resulted in higher accumulation of TCA cycle intermediates like isocitrate and fumarate in leaves of the susceptible genotype (TX86A5606). Lower grain number due to lesser productive spikes and reduced grain weight due to shorter grain-filling duration determined HNT-induced yield loss in winter wheat. Traits and mechanisms identified will help catalyze the development of physiological and metabolic markers for breeding HNT-tolerant wheat.

**KEYWORDS**

grain weight, high night-time temperature, metabolite profiling, night respiration, photosynthesis, winter wheat

## 1 | INTRODUCTION

Global climate models predict a mean temperature increase between 0.3°C and 4.8°C by the end of the 21st century (Intergovernmental Panel on Climate Change, 2014). Several studies have provided convincing evidence of a much faster increase in minimum night-time temperature compared with maximum day-time temperature (Alexander et al., 2006; Dai, Wigley, Boville, Kiehl, & Buja, 2001; Easterling et al., 1997; Sillmann, Kharin, Zhang, Zwiers, & Bronaugh, 2013). Further, frequent occurrence of warmer nights is considered a common global phenomenon (Vose, Easterling, & Gleason, 2005), with multimodel simulations predicting the increasing trend in night-time temperature to continue into the future (Sillmann, Kharin, Zhang, et al., 2013; Sillmann, Kharin, Zwiers, Zhang, & Bronaugh, 2013). Across most wheat-growing areas in the southern and northern hemisphere including the predominant wheat belt of Australia, North America, and Central and South Asia, impacts of warm nights have been documented even under current climatic conditions (Alexander et al., 2006; Fernandez-Long, Muller, Beltran-Przekurat, & Scarpati, 2013; Tank et al., 2006; Vincent & Mekis, 2006). Similarly, a recent modelling exercize involving an ensemble of 30 different wheat (*Triticum aestivum* L.) crop models confirms the negative impact of

  

warmer conditions on majority of the wheat-growing regions (Asseng et al., 2015). In addition, high night-time temperature (HNT) can potentially impact crop yields on large spatial regions and for longer periods, encompassing different growth and developmental phases unlike the short episodic occurrence of heat spikes during the day (Jagadish, Murty, & Quick, 2015). Hence, the future warmer climate poses a stiff challenge to sustain wheat productivity.

By virtue of its geographic and environmental adaptation, winter wheat is more sensitive to warming temperatures compared with other major cereals, including rice (Prasad, Bheemanahalli, & Jagadish, 2017). Four degree higher night-time temperature over ambient-using custom-designed chambers placed on bread wheat (variety - Baguette 13 Premium) grown under field condition, resulted in 3% and 4% reduction in 1,000 grain weight and grain yield, respectively (Garcia, Serrago, Dreccer, & Miralles, 2016). Evidence for negative relationship between grain yield and HNT in wheat comes from research in controlled environments (Narayanan, Prasad, Fritz, Boyle, & Gill, 2015), field conditions (Garcia et al., 2016; Garcia, Dreccer, Miralles, & Serrago, 2015), and modelling studies (Sillmann, Kharin, Zhang, et al., 2013; Sillmann, Kharin, Zwiers, et al., 2013). Hence, it is timely to unravel the mechanistic responses that induce tolerance to HNT, in an attempt to support ongoing efforts by the breeding community, aimed at developing heat stress resilient wheat.

Carbon balance in crops, including wheat, hinges on the dynamics between photosynthesis (Net $CO_2$ assimilation) and night-time respiration, which can be altered considerably depending on the prevailing climatic conditions and the crop growth stage. Wheat, like other crops, fixes carbon through photosynthesis and releases the assimilated carbon through respiration, primarily night respiration, which determines the crop carbon balance. By estimating the diurnal variation in respiration at every 2-hr intervals, Swain, Baig, and Naik (2000) recorded the lowest respiration during midday and higher levels at dawn and dusk in rice (*Oryza sativa*) leaves, indicating higher respiratory carbon losses during night-time. Respiration is responsible for up to 70% carbon loss from carbon fixed by daily photosynthesis (Atkin, Bruhn, Hurry, & Tjoelker, 2005; Atkin, Scheurwater, & Pons, 2007; Atkin & Tjoelker, 2003; Liang, Xia, Liu, & Wan, 2013).

Moreover, the proportion of carbon used for night respiration increases during early to mid-grain filling, which coincides with both senescence and higher range of temperatures that wheat experiences under current growing conditions (Lobell, Sibley, & Ortiz-Monasterio, 2012; Sakuraba et al., 2014; Singh et al., 2015). This leads to quicker break-down of stored assimilates due to increased respiration, which would otherwise contribute towards grain filling. Genetic diversity for night-respiration has been reported in cereals (Bahuguna, Solis, Shi, & Jagadish, 2017; Peraudeau et al., 2015), including wheat (Pinto, Molero, & Reynolds, 2017). Different mechanistic routes inducing yield loss such as increased spikelet sterility under high day-time temperature and reduced plant carbohydrate pool, biomass, and increased postflowering night respiration under HNT exposure have been prominently demonstrated in rice (Bahuguna et al., 2017; Jagadish et al., 2015; Shi et al., 2013; Shi et al., 2016). Few studies have investigated the effect of HNT on wheat yield and have revealed shorter critical growth period, higher dark-respiration, lower leaf photosynthesis, decreased antioxidant capacity, lower biomass, lower grain number, and seed-set as the major determinants of yield loss under HNT (Garcia et al., 2015; Narayanan et al., 2015; Pinto et al., 2017). Further, Garcia et al. (2016) concluded that postanthesis HNT-induced yield loss in wheat is directly related to processes within the grain itself rather than an impact on the availability of assimilates. Although there have been efforts to understand HNT-induced changes in physiological, growth, and yield related traits in wheat, the metabolic changes responsible for HNT-induced responses are yet to be identified. Metabolite profiling is one of the important tools to identify heat stress-induced alterations in biochemical pathways, which would help identify by-products of stress metabolism, stress signal transduction, and molecules that impart tolerance and acclimation responses (Kaplan et al., 2004; Shulaev, Cortes, Miller, & Mittler, 2008). Metabolite profiles of rice leaves exposed to HNT revealed activation of the TriCarboxylic Acid (TCA) cycle and amino acid biosynthesis, particularly in sensitive genotypes (Glaubitz et al., 2017; Glaubitz, Erban, Kopka, Hincha, & Zuther, 2015). In rice, sugar metabolism was found to regulate floral organ tolerance or susceptibility to heat and drought stress (Li et al., 2015). Similarly, in wheat leaves, metabolites such as sugars, organic acids, and amino acids were altered in abundance under drought stress, with an increase in proline, methionine, arginine, lysine, aromatic, and branched-chain amino acids in the sensitive genotype (Michaletti, Naghavi, Toorchi, Zolla, & Rinalducci, 2018).

In spite of the growing evidence supporting HNT-induced yield and quality losses, literature on night respiration, carbon balance, and the mechanistic basis of tolerance in crops is limited. This is particularly the case with information on carbon balance during the critical postflowering phase in winter wheat. Hence, to fill this major knowledge gap, we aim to (a) assess the impact of HNT on grain yield and yield-related traits; (b) determine temporal changes in carbon balance under HNT exposure during grain filling and its impact on yield and related traits; and (c) unravel metabolic changes in the source (leaf), sink (spike), and transport (stem) tissue that induce HNT tolerance in winter wheat.

## 2 | MATERIALS AND METHODS

The experiments were carried out in controlled environment chambers at the Department of Agronomy, Kansas State University, Manhattan, Kansas in 2016. Experiment 1 (Exp. 1) included six winter wheat genotypes selected from an earlier screening of 300 diverse winter wheat Coordinated Agricultural Project panel for seedling stage abiotic stress tolerance. These selected six winter wheat genotypes, Tascosa, Guymon, and Gage—seedling stage salinity tolerant genotypes and Carson, 2174-05, and TX86A5606—seedling stage salinity sensitive genotypes (Ehtaiwesh, 2016), were tested for post-heading HNT stress responses (Supplementary Table S1). The seeds of these six winter wheat genotypes were obtained from the Germplasm Resources Information Network database. Based on the results from Exp. 1, two genotypes (Tascosa and TX86A5606) with contrasting night respiration under HNT were validated for physiological responses and for identifying source (leaf), sink (spike), and transport (stem) tissue metabolic changes in Experiment 2 (Exp. 2).

## 2.1 | Plant growth

Seeds were sown in 30.5 × 61-cm seeding trays filled with Sunshine Metro-Mix 380 potting mix (SunGro Horticulture, Agawam, MA). The trays were maintained in controlled environment chambers at 26/15°C maximum-day and minimum-night temperatures, respectively, with a photoperiod of 16 hr light and 8 hr dark for a week. After emergence of most of the seedlings, the seeding trays were transferred to vernalization chambers set at 4°C for 6 weeks. Following vernalization, trays with the seedlings were transferred back to controlled environment chambers maintained at 20°/15°C maximum-day and minimum-night temperatures for a week. The seedlings were then transplanted (two seedlings/pot) in to 1.6-L (10 × 24 cm, MT49 Mini-Treepot) capacity pots filled with Sunshine Metro-Mix 380 potting mix. Before transplanting, each pot was fertilized with 5 g of Scotts Osmocote classic (14–14-14 of N-P-K) and 0.5 g of Scotts Micromax Micronutrients (Hummert International, Topeka, KS). After transplanting, the pots were arranged in trays and placed in controlled environment chambers (chamber dimensions of 1.52 m wide, 2.45 m long, and 2.15 m high in Exp. 1; and 0.79 m wide, 1.82 m long, and 1.85 m high in Exp. 2) maintained at 26/15°C maximum-day/minimum-night temperatures. The plants were well-watered throughout the experiment, wherein about 1-cm water layer was maintained in trays holding the pots. Marathon 60 WP (insecticide, OHP) was applied to the soil after 2 weeks of transplanting to avoid infestation by sucking pests. Avid 0.15EC (insecticide, Syngenta) and Strike Plus 50 WDG (fungicide, OHP) were sprayed on plants to prevent mite and powdery mildew infestation, respectively, at grain-filling stage.

The main tiller in each plant was tagged on the day heading began and a half of the plants (15 and 60 plants per genotype in Exp. 1 and Exp. 2, respectively) were transferred to three HNT chambers maintained at 26/23°C maximum-day/minimum-night temperatures. Five and 20 plants per genotype were placed in each of the three replicate chambers in Exp. 1 and Exp. 2, respectively. The other half of the plants remained in three control treatment chambers maintained at 26/15°C maximum-day/minimum-night temperatures. Both control and HNT chambers were maintained at 16/8 hr (day/night) photoperiod, with 900–1,000 μmol $m^{-2}$ $s^{-1}$ light intensity at 5 cm above the canopy and 70% relative humidity (RH). Maximum and minimum temperatures were maintained for 8 hr each in all growth chambers with a transition period of 4 hr between maximum-day and minimum-night temperatures. Temperature and RH at canopy level were recorded every 30 min using HOBO UX 100–011 temperature/RH data loggers (Onset Computer Corp., Bourne, Massachusetts) in all growth chambers, in both the experiments.

## 2.2 | Observations and sampling

### 2.2.1 | Photosynthesis and night respiration measurements

Net $CO_2$ assimilation or photosynthesis during the day and respiration during the night were recorded from flag leaves on tagged main tiller using LI-6400XT portable photosynthesis system (LI-COR Biosciences, Lincoln, NE, USA). The Net $CO_2$ assimilation measurements were taken with a portable photosynthesis system set at a block temperature of 26°C, with leaf chamber $CO_2$ fixed at 400 ppm with a flow rate of 500 μmol $s^{-1}$ and a light intensity of 1,000 μmol $m^{-2}$ $s^{-1}$ of Photosynthetically Active Radiation (PAR) supplied by red-blue light emitting diode. Night-respiration measurements were recorded with the same portable photosynthesis system set at a block temperature of 15°C and 23°C in control and HNT treatments, respectively. The leaf chamber $CO_2$ was fixed at 400 ppm with a flow rate adjusted to 100 μmol $s^{-1}$ following the instruction manual to minimize fluctuations. Care was taken to avoid exposure to external sources of PAR, which was confirmed by Light Sensor Reader and 6 Sensor Quantum Bar (field scout and light scout; Spectrum Technologies, Inc., Aurora, IL, USA), prior to initiating night respiration measurements. In Exp. 1, to identify the time of stable photosynthesis and peak night respiration for each genotype, diurnal leaf carbon exchange measurements were recorded every 2 hr starting 4 days after heading (DAH) or stress imposition. On the fourth DAH, photosynthesis was recorded at 07, 09, 11, 13, 15, 17, and 19 hr and night respiration recorded at 21, 23, 01, 03, and 05 hr. Once the time of stable assimilation and peak night respiration were obtained, all subsequent measurements for photosynthesis and night respiration were recorded at the peak time periods between 09 to 11 hr and 23 to 01 hr, respectively, once every 4 days starting 4 DAH until 28 DAH in all six genotypes. Peak night-respiration period was selected to record the maximum carbon loss induced under HNT in a genotype, to capture respiration differing significantly between control and stress conditions. Based on the night respiration data recorded in Exp. 1, two genotypes with contrasting night-respiration responses under HNT were selected for validation in Exp. 2. Photosynthesis and night respiration were recorded at the peak time periods (between 09 to 11 hr and 23 to 01 hr) on 2, 4, 6, 8, 12, 20, and 24 DAH in two contrasting genotypes in Exp. 2. Photosynthesis and night respiration measurements were initiated at 09 h and 23 h, respectively; and in most days, measurements were completed within 45 min except on few days when there were more plants to measure.

### 2.2.2 | Growth and yield parameters

At physiological maturity (Zadoks growth scale 9-Ripening [92-Grain hard, not dented by thumbnail]), yield and yield components were recorded. Plant height (cm) was measured from the bottom of the stem until the tip of the spike without considering the awns in three random tillers in a plant. Other growth parameters, including total number of tillers per plant and total number of productive spikes per plant, were recorded at harvest. The plants were hand-harvested and all the yield and yield components were recorded as follows: (a) leaves and stems were dried in forced air drier at 60°C for about 15 days, and constant weights were recorded to obtain the shoot dry weight; (b) spikes were dried at 40°C for 7 days before threshing using a wheat head thresher (Precision Machine Co., Lincoln, Nebraska); and (c) grain weight per plant and 1,000 grain weight were recorded, with total number of grains per plant counted manually.

### 2.2.3 | Metabolite profiling

Plant samples were collected on 2, 4, 6, 8, and 12 DAH in both the genotypes grown under control and HNT treatments, between 23 to 01 hr immediately after night-respiration measurements were recorded in each plant in Exp. 2. All the leaves, stems, and spikes were collected from three replicate plants and were immediately frozen in liquid nitrogen and stored at −80°C. Frozen samples were ground to fine powder using liquid nitrogen and aliquoted to gain 50 mg of the powder. Metabolites were extracted by methanol/water/chloroform as described in Lisec, Schauer, Kopka,Willmitzer, & Fernie, (2006) and 200 µl of the upper aqueous phase was dried in a vacuum concentrator. Dried metabolite pellets were subjected to derivatization by methoxyamine hydrochloride (Sigma) and N-Methyl-N-(trimethylsilyl) trifluoroacetamide (Sigma) as described in Lisec, Schauer, Kopka, Willmitzer, and Fernie (2006). Metabolite profiling was performed by 5977A GC/MSD (Agilent) with parameters following Lisec et al. (2006) except for the MS scan rate that was adjusted to five scans per second. Peaks were manually annotated and ion intensity was determined through TagFinder (Luedemann, von Malotky, Erban, & Kopka, 2012) using a reference library derived from Golm-Metabolome-Database (Kopka et al., 2005). The parameters used for peak annotation are shown in Supplementary Tables S2 & 3, following the recommended reporting format (Fernie et al., 2011). The peak intensity of a selected ion was normalized to that of the internal standard (ribitol) and fresh weight of the material. Values were further normalized by the mean of all Day 2 samples for each metabolite to calculate relative levels of metabolites on all other sampling points (Supplementary Table S4).

### 2.2.4 | Statistical analysis

The experiments were laid out in a split plot randomized complete block design with temperature as the main-plot factor and genotype as the subplot factor with three independent chamber replications for control and HNT in both the experiments. Two-way analysis of variance (ANOVA) for all the growth and yield parameters was performed using PROC GLM procedure in SAS software (Version 9.4, SAS Institute). Repeated measures ANOVA for photosynthesis and night-respiration measurements recorded over different days were performed using PROC MIXED procedure in SAS software (Version 9.4, SAS Institute). Means were separated using least significant difference test at $p = 0.05$. Partial least square discrimination analysis (PLS-DA) was done on the metabolite profiling data, for each tissue (spike, leaf, and stem) separately, to reduce the dimensionality of the data and to classify temperature groups using MetaboAnalyst 4.0 software (http://www.metaboanalyst.ca/). Repeated measures ANOVA was carried out on the entire normalized metabolite profiling data to identify a significant effect of treatment, genotype, and days after heading and their interactions on metabolites using PROC MIXED procedure in SAS software (Version 9.4, SAS Institute). The metabolic pathways altered under HNT stress were identified using Metabolomics tool for Pathway Analysis (MetPA), a web-based tool incorporated into MetaboAnalyst platform (Michaletti et al., 2018; Xia & Wishart, 2010). MetPA module combines results of pathway enrichment analysis with pathway topology analysis. Data for all the metabolites with significant ($p \leq 0.05$) temperature, Temperature × Genotype and Temperature × Genotype × DAH interaction effects were submitted to MetPA independently for each tissue with annotation based on common chemical names. Verification of accepted metabolites was conducted manually using human metabolome database, Kyoto Encyclopedia of genes and genomes, and PubChem databases. *O. sativa* pathway library was used for pathway analysis. Globaltest pathway enrichment analysis method was followed and raw *p*-values <0.05 indicated significant enrichment of metabolites in a pathway. Because many pathways are tested at the same time, the statistical *p*-values from enrichment analysis were further adjusted via false discovery rate (FDR) estimation. Pathway topology analysis considers structural information of pathways to identify the positions of change and their relative impact on the pathway. The "importance measure" of each metabolite is the percentage with respect to the total pathway importance, and the pathway impact is the cumulative percentage from all the altered metabolites.

## 3 | RESULTS

### 3.1 | Growth and yield parameters

HNT induced early senescence leading to early maturity in most of the tested genotypes (Figure 1a,b). Days to physiological maturity were significantly affected by temperature (T), genotype (G), and T × G interaction ($p < 0.05$). HNT advanced maturity by 11 days in 2174-05 and 8 days in Guymon over control, whereas Carson was minimally affected by HNT (Figure 1a). Plants in Exp. 2 exhibited lower growth resulting in lower shoot and grain weight compared with Exp. 1, irrespective of the treatments (Table 1), which could possibly be due to the use of smaller growth chambers during vegetative phase in Exp. 2 compared with Exp. 1. Growth and yield parameters were significantly affected by T and G in Exp. 1 with significant T × G interaction effect recorded with grain yield, spike weight, and number of productive spikes (Table 1; Supplementary Table S5). When averaged across genotypes, HNT induced 66% and 26% reduction in grain yield and thousand grain weight over control, respectively. Highest percent reduction in grain yield under HNT over control was recorded in 2174-05 (81%), followed by Carson (74%), whereas Gage (55%) and Tascosa (59%) recorded lower percent reductions (Table 1). In Exp. 2, a significant effect of T was observed for all the growth and yield parameters measured except for number of tillers per plant (Table 1; Supplementary Table S5). Whereas, significant genotypic effect was recorded only for shoot dry weight per plant with no significant interaction between genotype and temperature for any of the measured traits (Table 1; Supplementary Table S5). In Exp. 2, grain yield was reduced by 41% and 66% in Tascosa and TX86A5606, respectively, under HNT compared with control. Thousand kernel weight under HNT exposure was reduced by 12% and 23% in Tascosa and TX86A5606 over control, respectively (Table 1).

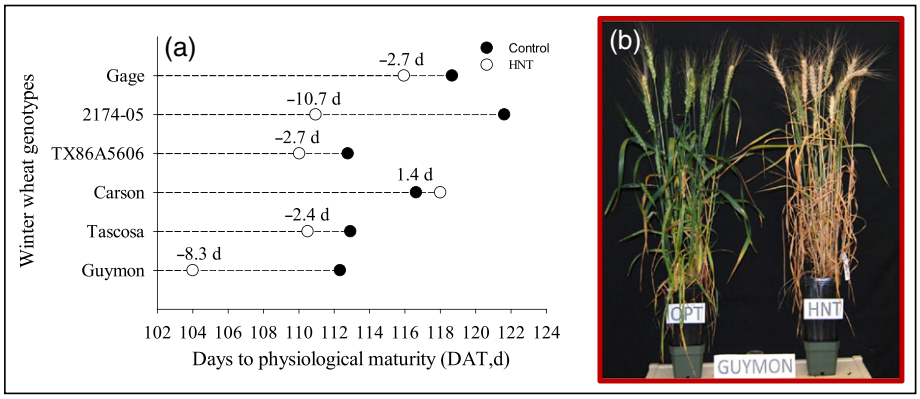


**FIGURE 1** Days to physiological maturity (a) of six winter wheat genotypes grown under control (26/15°C) and high night-time temperature (HNT; 26/23°C) treatments in Experiment 1 (Exp. 1). (b) Genotype Guymon grown under control and HNT treatments in Exp. 1. Days after transplanting (DAT)

**TABLE 1** Shoot dry weight (g plant$^{-1}$), grain yield (g plant$^{-1}$), number of grains (plant$^{-1}$), and thousand kernel weight (g) of winter wheat genotypes grown under control and high night-time temperature (HNT) treatments in Experiments 1 and 2. Values in italics are probability (p) for temperature (T), genotype (G), and their interaction (T × G) effects for respective traits

| Genotypes | Shoot dry weight (g plant$^{-1}$) | | Grain yield (g plant$^{-1}$) | | Grain number (plant$^{-1}$) | | Thousand kernel weight (g) | |
|---|---|---|---|---|---|---|---|---|
| | Control | HNT | Control | HNT | Control | HNT | Control | HNT |
| Experiment 1 | | | | | | | | |
| Guymon | 13.5 ± 0.5 | 11.5 ± 0.5 | 21.6 ± 2 | 8.5 ± 1 | 673 ± 50 | 390 ± 56 | 32.7 ± 2 | 21.8 ± 1 |
| Tascosa | 25.4 ± 2 | 24.8 ± 2 | 19.8 ± 1 | 8.1 ± 1 | 504 ± 20 | 237 ± 20 | 39.3 ± 1 | 32.9 ± 2 |
| Carson | 30.0 ± 3 | 16.2 ± 1 | 33.1 ± 2 | 8.6 ± 1 | 856 ± 82 | 297 ± 34 | 39.5 ± 1 | 28.8 ± 2 |
| TX86A5606 | 11.4 ± 1 | 8.2 ± 0.7 | 24.0 ± 1 | 7.9 ± 0.7 | 554 ± 37 | 243 ± 20 | 43.8 ± 2 | 33.0 ± 2 |
| 2174-05 | 11.5 ± 0.6 | 6.7 ± 1 | 15.6 ± 1 | 3.0 ± 0.5 | 441 ± 23 | 130 ± 18 | 35.5 ± 1 | 22.7 ± 2 |
| Gage | 37.1 ± 3 | 30.1 ± 2 | 30.9 ± 3 | 14.0 ± 1 | 852 ± 93 | 482 ± 43 | 36.1 ± 1 | 28.6 ± 1 |
| T | *<0.001* | | *<0.0001* | | *<0.001* | | *<0.001* | |
| G | *<0.001* | | *<0.0001* | | *<0.001* | | *<0.001* | |
| T × G | *0.0835* | | *0.0012* | | *0.0598* | | *0.2717* | |
| Experiment 2 | | | | | | | | |
| Tascosa | 16.9 ± 3 | 8.1 ± 2 | 14.5 ± 2 | 8.5 ± 2 | 450 ± 70 | 288 ± 65 | 32.5 ± 2 | 28.5 ± 2 |
| TX86A5606 | 10.0 ± 0.6 | 3.8 ± 0.6 | 20.8 ± 2 | 7.0 ± 1 | 534 ± 46 | 228 ± 36 | 39.0 ± 1 | 30.0 ± 2 |
| T | *0.0025* | | *0.0052* | | *0.0109* | | *0.0237* | |
| G | *0.0132* | | *0.3658* | | *0.8513* | | *0.0822* | |
| T × G | *0.2642* | | *0.2031* | | *0.3521* | | *0.4257* | |

## 3.2 | Net $CO_2$ assimilation (photosynthesis) and night respiration

To identify the time-of-day with maximum net carbon assimilation and time-of-night with peak night respiration, diurnal gas-exchange measurements were recorded on flag leaves 4 DAH or stress exposure in Exp. 1. Net $CO_2$ assimilation measured at every 2 hr intervals from 0700 hr to 1900 hr, recorded significant ($p < 0.05$) genotype (G), temperature (T) x genotype (G), time of day (D), T × D, and G × D interactions. In both control and HNT treatment, an increasing trend in net $CO_2$ assimilation was noticed as the day progressed, with maximum and stable net $CO_2$ assimilation recorded between 09 to 11 hr in many of the tested genotypes (Figure 2). Night respiration measured at every 2-hr intervals from 21 hr to 05 hr on the fourth night of stress exposure, recorded a significant ($p < 0.01$) T, G, D, T × G, T × D, G × D, and T × G × D interaction effect. On average, HNT increased night respiration significantly ($p < 0.05$) over control treatment. The increase in night respiration with HNT was at the maximum between 23 hr to 01 hr in many of the tested genotypes (Figure 2). Genotypes "Gage" and "Tascosa" did not show any increase in night respiration throughout the night. Based on the above results, all subsequent temporal photosynthesis and night-respiration measurements were recorded between 09 hr to 11 hr and 23 hr to 01 hr, respectively.

In Exp. 1, temporal net $CO_2$ assimilation measurements recorded throughout the grain-filling period on every fourth day starting at 4 DAH until 28 DAH were significantly ($p < 0.05$) affected by G, T × G, D, G × D, and T × G × D interactions. Net $CO_2$ assimilation recorded a decreasing trend over time in all the tested genotypes (Figure 3). This decreasing trend was significantly faster in plants

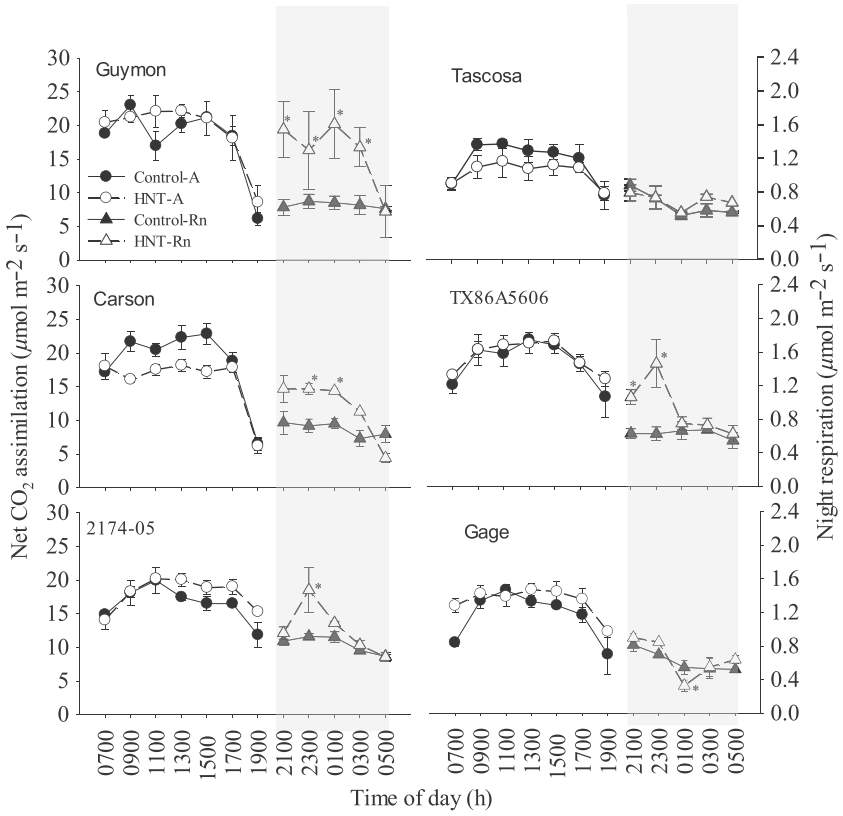


**FIGURE 2** Diurnal net $CO_2$ assimilation and night respiration in flag leaves of six winter wheat genotypes, at 4 days after heading in control and high night-time temperature treatments in Experiment 1. *indicates significant difference between treatment means at $p \leq 0.05$. A = Net $CO_2$ assimilation, Rn = Night respiration. Night time or dark periods are shaded with grey

exposed to HNT compared with control during the late grain-filling phase, especially in genotypes like Guymon and TX86A5606 (Figure 3). On the other hand, temporal night-respiration measurements were significantly affected by G, D, T × D, and G × D interactions. Genotypes Carson (59%), TX86A5606 (133%), and 2174-05 (64%) recorded an increase in night respiration under HNT over control at 4 DAH exposure, but a sustained increase was not noticed at 8 DAH and beyond (Figure 3). Tascosa and Gage did not record an increase in night respiration under HNT over control throughout the grain-filling period. In order to validate the contrasting night-respiration responses in genotypes exposed to HNT from Exp. 1, genotype Tascosa with no increase in night respiration and TX86A5606 recording the highest increase in night respiration were selected. In Exp. 2, involving Tascosa and TX86A5606, a significant ($p < 0.05$) T × G × D interaction effect was recorded for both net $CO_2$ assimilation and night respiration. Similar to Exp. 1, a decrease in net $CO_2$ assimilation over time with rapid reduction under HNT was noticed during late grain-filling phase in Exp. 2 (Figure 4). In Tascosa, there was no increase in night-respiration under HNT over control except at 12 DAH. However, HNT induced a significant increase in night respiration over control at 4 and 6 DAH in TX86A5606. Similar to Exp. 1, HNT-induced increase in night respiration was not noticed at 8 DAH and beyond (Figure 4).

## 3.3 | Differential metabolite accumulation in spikes, leaves, and stems

Metabolite profiling analysis was carried out on spike, leaf, and stem tissues of Tascosa and TX86A5606 from Exp. 2 with 47, 61, and 56 metabolites detected in spike, leaf, and stem tissues, respectively (Supplementary Table. S4). PLS-DA was performed to visualize treatment-induced changes in metabolite profile in spike, leaf, and stem (Supplementary Figure S1). The results show an overlap among spike samples exposed to control and HNT (Supplementary Figure S1A), whereas the same in leaves and stem had little to no overlap (Supplementary Figure S1B and C). Repeated measures ANOVA was carried out on metabolite data to identify the metabolites that had significant (a) Temperature (T), (b) T × G (genotype), and (c) T × G × DAH interaction effect. Night-time temperature had a significant ($p \leq 0.05$) effect on nine, 11 and eight metabolites in spike, leaf, and stem, respectively (Supplementary Table S6). In spikes, six metabolites including three sugars, two amino-acids, and one nucleobase (uracil) were significantly ($p \leq 0.01$) increased under HNT (Figure 5A). In leaves, three metabolites including alanine, fumarate, and isocitrate increased under HNT compared with control, whereas three other metabolites (quinic acid, adenine, and glycine) decreased under HNT at $p \leq 0.01$ significance (Figure 5b). In contrast, all five amino acids in stem were significantly ($p \leq 0.01$) lower under HNT compared with control (Figure 5c). Significant T × G interaction effects ($p \leq 0.05$) were recorded for 11, 10, and five metabolites in spike, leaf, and stem tissues, respectively (Supplementary Table S6). In spike, sugars (sucrose, glucose, and fructose), myo-inositol, pyroglutamate, and phosphate recorded a significant ($p < 0.01$) increase under HNT in Tascosa compared with control, whereas the same metabolites were decreased under HNT in TX86A5606 compared with control (Figure 6a). However, amino acid glycine increased under HNT stress in spikes irrespective of the genotype (Figure 6a). Leaf amino acids including lysine, leucine, and tyrosine decreased ($p < 0.01$) under HNT in Tascosa and increased under HNT in TX86A5606, compared

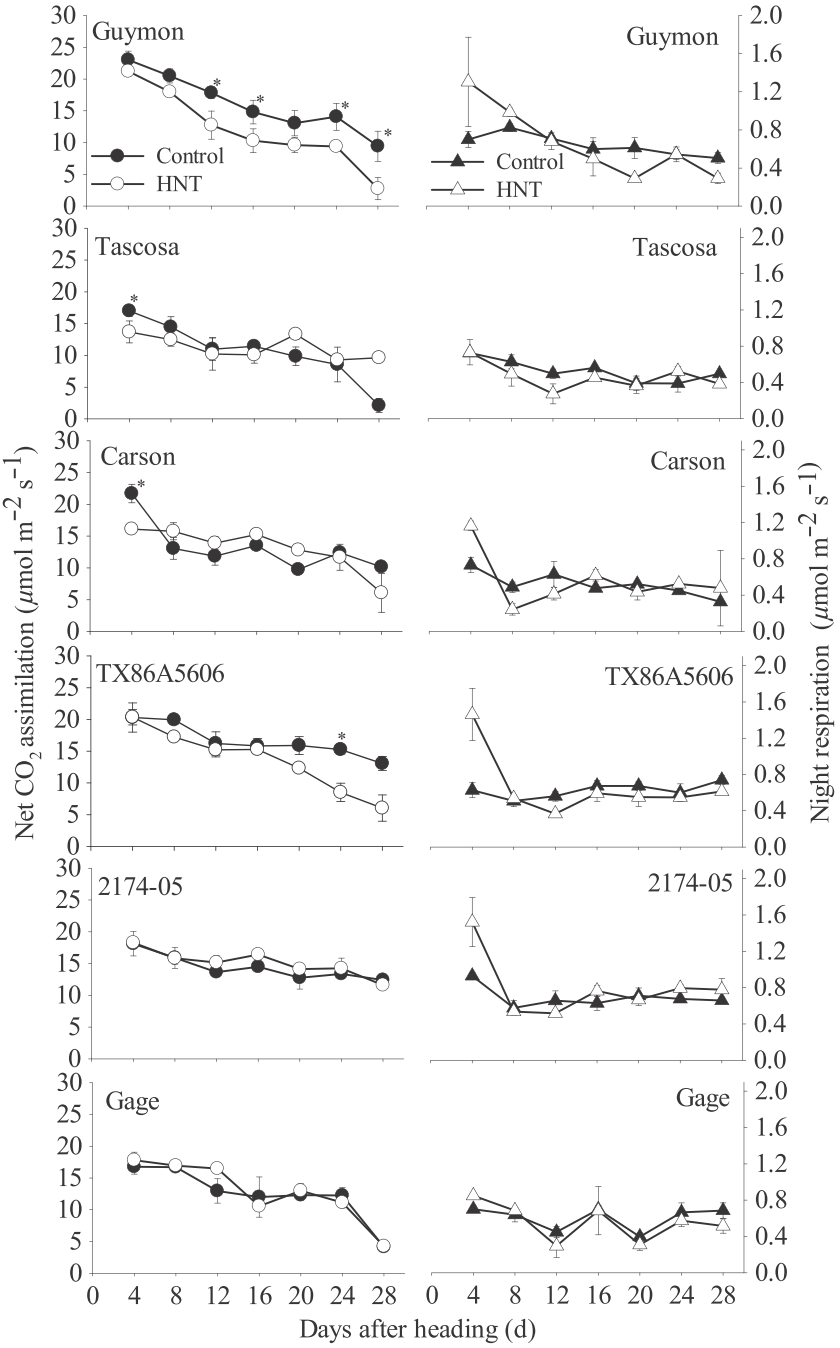


**FIGURE 3** Net $CO_2$ assimilation and night respiration during grain filling phase in flag leaves of six winter wheat genotypes grown under control and high nigh-time temperature (HNT) treatments in Experiment 1. * indicates significant difference between treatment means at $p \leq 0.05$

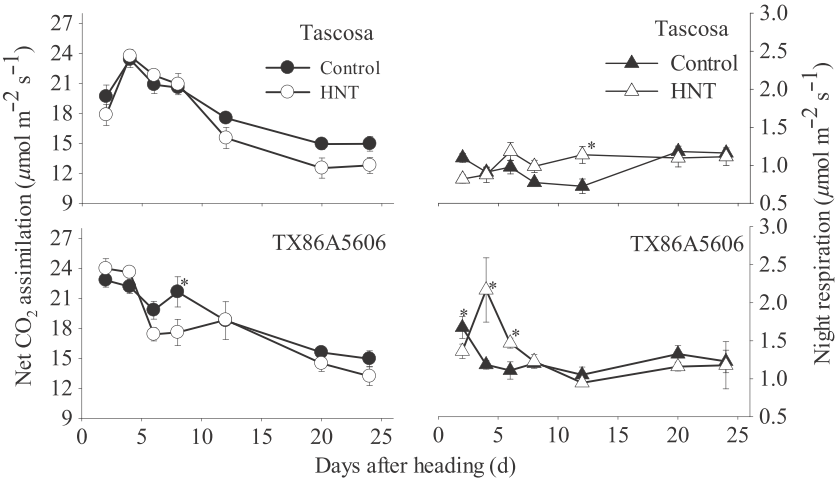


**FIGURE 4** Net $CO_2$ assimilation and night respiration during grain-filling phase in flag leaves of two winter wheat genotypes grown under control and high nigh-time temperature (HNT) treatments in Experiment 2. * indicates significant difference between treatment means at $p \leq 0.05$

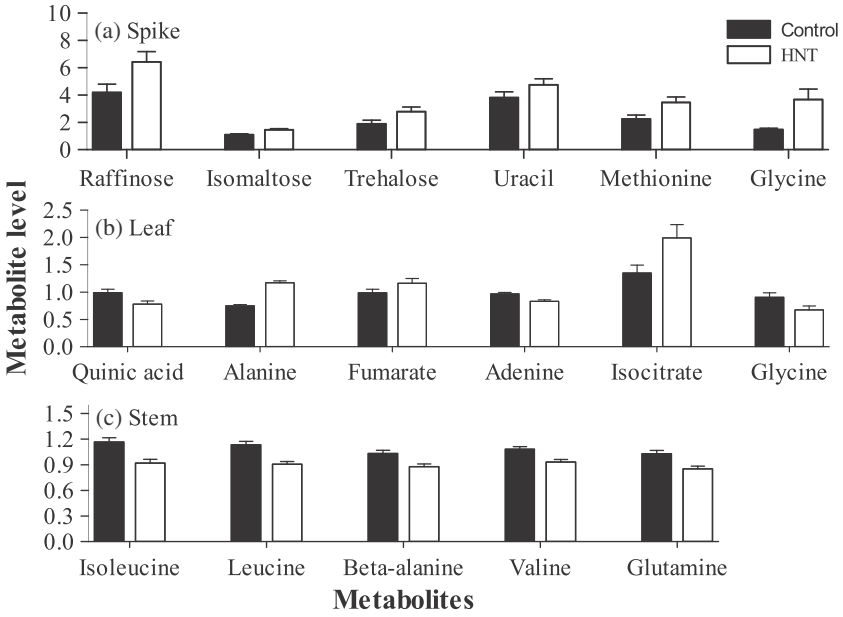


**FIGURE 5** Night-time temperature responsive metabolites in (a) spikes, (b) leaves, and (c) stems of two contrasting winter wheat genotypes under control and high night-time temperature stress (HNT). Metabolites with significant temperature effect at $p \leq 0.01$ based on repeated measures analysis of variance are represented in the graph. Bars represent normalized values averaged across replications, genotypes, and days after stress ± standard error ($n$ = 30)

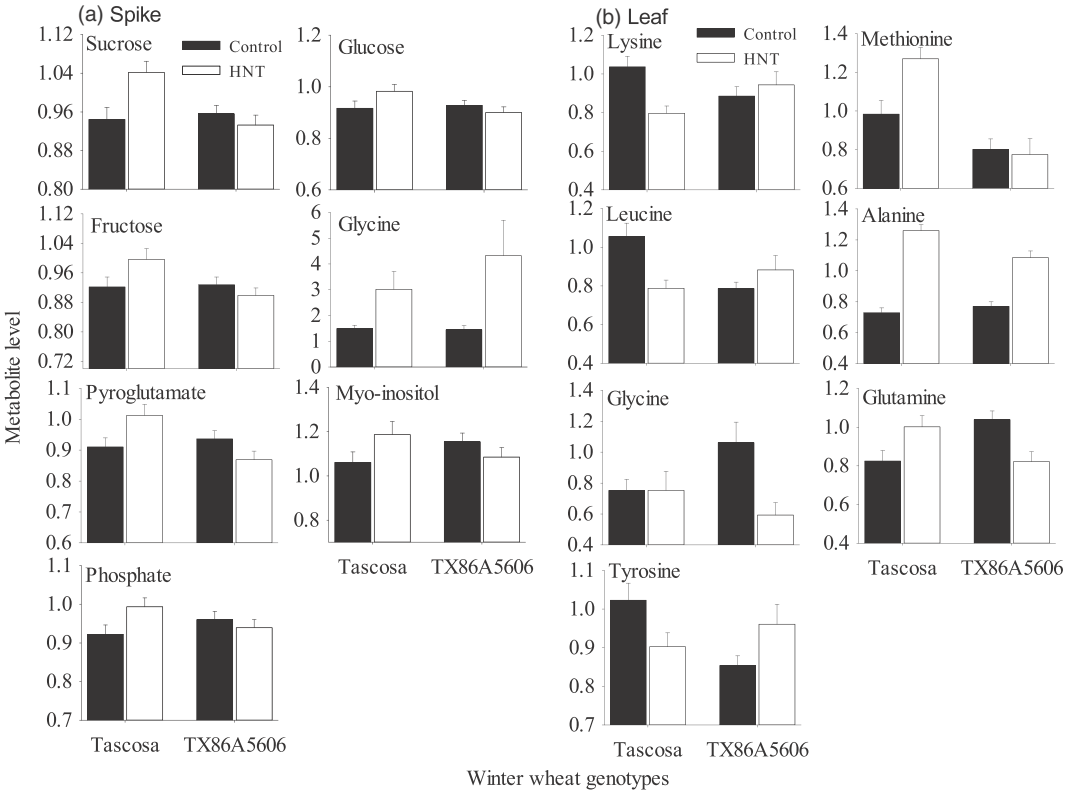


**FIGURE 6** Metabolites with differential accumulation in tolerant and sensitive genotypes under control and high night-time temperature stress (HNT). Metabolites with significant Temperature × Genotype interaction effect at $p \leq 0.01$ based on repeated measures analysis of variance are presented in the graph. Bars represent normalized values averaged across replications and days after stress ± standard error ($n$ = 15)

with control (Figure 6b). Methionine and glutamine increased in Tascosa although both recorded a decrease in TX86A5606 leaves under HNT compared with control (Figure 6b). Alanine accumulation was higher under HNT in leaves of both the genotypes but glycine recorded a significant reduction under HNT only in TX86A5606 leaves (Figure 6b). Interestingly, a three-way significant interaction (T × G × DAH) was recorded for 10, eight, and three metabolites in spike, leaf, and stem tissue, respectively (Supplementary Table S6). In spikes, some of the metabolites like glycerol, glycerol 3 phosphate, glycerate, and beta-alanine recorded an increase in TX6A5606 under HNT at 4DAH, with a gradual decline after 4 DAH (Figure 7a). Amino acids alanine and glycine recorded an

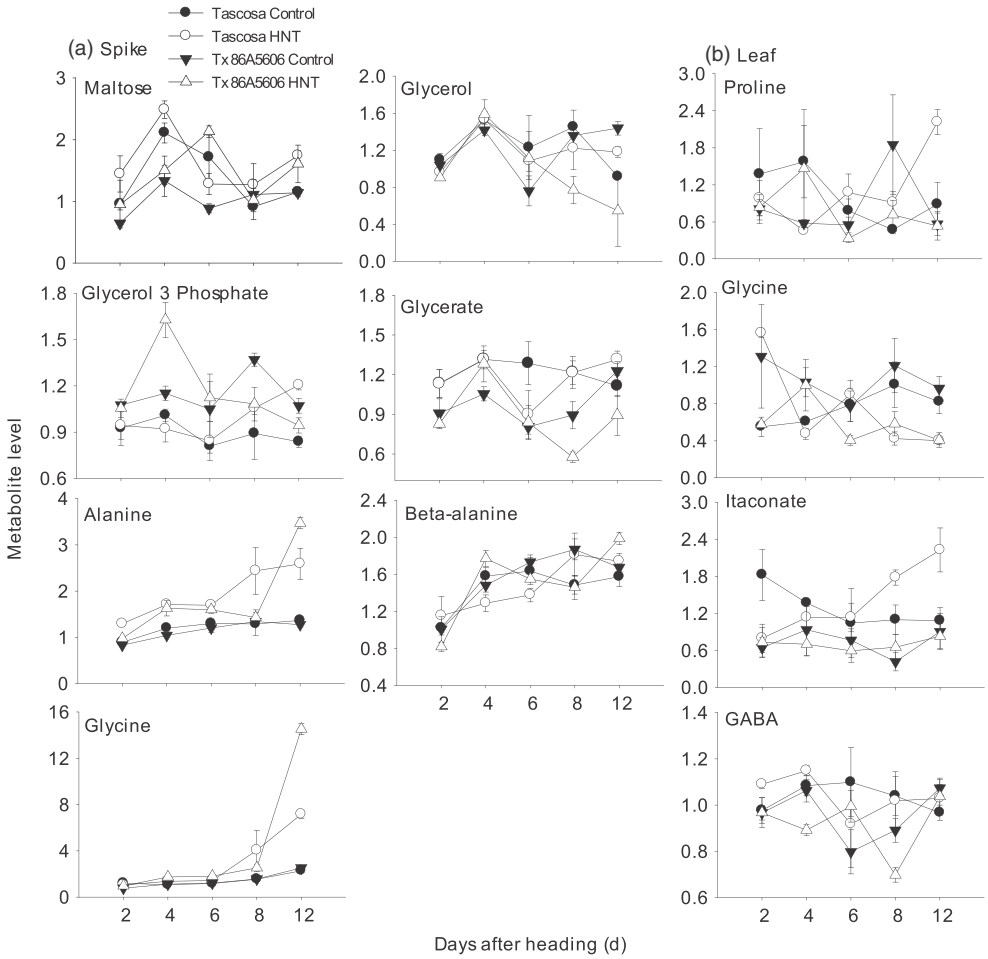


**FIGURE 7** Genotype specific and night-time temperature responsive metabolites over different days during grain filling under control and high night-time temperature stress (HNT). Metabolites with significant Temperature × Genotype × Days after stress interaction effect at $p \leq 0.01$ are presented in the graph. Symbols represent mean of normalized values ± standard error ($n = 3$)

increase as the stress progressed in spikes of both genotypes with a greater increase in TX86A5606 than Tascosa at 12 DAH (Figure 7 a). An increase in proline and itaconate accumulation was seen in leaves of Tascosa as the HNT stress progressed over time, whereas a similar increase was not seen with TX86A5606 (Figure 7b). A decrease in glycine accumulation was recorded in leaves of both the genotypes as the stress progressed. Higher accumulation of gamma-aminobutyric acid, was recorded in Tascosa compared with TX86A5606 under both the temperature treatments (Figure 7b). Most significantly altered pathways under HNT are presented in Supplementary Table S7. Pathway topology analysis revealed pathways 5, 1, and 4 to be significantly (FDR < 0.05; impact value >0.1) altered in response to HNT in spike, leaf, and stem, respectively (Supplementary Table S7). Functionally important metabolic pathways and significant metabolites within these pathways having major impact in spikes when challenged with HNT are as follows: (a) glycine, serine, and threonine metabolism (with a significant increase in glycine under HNT); (b) alanine, asparate, and glutamate metabolism (with a significant decrease in aspartate under HNT); (c) cysteine and methionine metabolism (with a significant increase in methionine under HNT); (d) starch and sucrose metabolism (with a significant increase in maltose under HNT); and (e) galactose metabolism (with a significant increase in raffinose under HNT) (Table 2). Alanine, aspartate, and glutamate metabolism (with a significant decrease in stem glutamine) emerged as one of the key pathways with high impact under HNT in both leaf and stem (Table 2). In addition, in stem (a) beta-alanine metabolism (with a significant decrease in beta-alanine), (b) pantothenate and CoA biosynthesis with a significant decrease in beta-alanine and (c) arginine and proline metabolism emerged as pathways having higher impact under HNT exposure (Table 2).

## 4 | DISCUSSION

### 4.1 | Implications of HNT on yield parameters (Objective 1)

In wheat, kernel weight is mainly determined by rate and duration of grain filling and translocation of stored preanthesis assimilates to the developing grain (Calderini, Savin, Abeledo, Reynolds, & Slafer, 2001). Postanthesis abiotic stresses like drought and heat stress reduce the duration of effective grain filling and also negatively affect the current photosynthetic activity, resulting in poor grain filling and

**TABLE 2** Pathways with high impact values with the metabolites that altered under HNT. Metabolites with significant *p*-value and high importance are highlighted in bold. Importance values are given based on position of altered metabolite and their relative impact within the pathway

| Tissue | Metabolism | Metabolite | p value | Importance | Changes under HNT over control |
|---|---|---|---|---|---|
| Spike | Glycine, serine, and threonine metabolism | **Glycine** | 0.005 | 0.217 | Increased |
| | | Serine | 0.347 | 0.180 | Increased |
| | | Homo serine | 0.488 | 0.076 | Decreased |
| | | Aspartate | 0.019 | 0 | Decreased |
| | Alanine, aspartate, and glutamate metabolism | **Aspartate** | 0.019 | 0.240 | Decreased |
| | | Alanine | <0.001 | 0 | Increased |
| | | GABA | 0.321 | 0 | Decreased |
| | Cysteine and methionine metabolism | **Methionine** | 0.017 | 0.174 | Increased |
| | | Serine | 0.347 | 0 | Increased |
| | | Homo serine | 0.489 | 0 | Decreased |
| | | Aspartate | 0.019 | 0 | Decreased |
| | Starch and sucrose metabolism | Glucose | 0.360 | 0 | No change |
| | | **Maltose** | 0.018 | 0.081 | Increased |
| | | Sucrose | 0.895 | 0.027 | No change |
| | | Fructose | 0.309 | 0.004 | No change |
| | Galactose metabolism | Glycerol | 0.129 | 0 | Decreased |
| | | **Raffinose** | 0.022 | 0.045 | Increased |
| | | Sucrose | 0.895 | 0.037 | No change |
| | | Glucose | 0.360 | 0.021 | No change |
| | | Myo-inositol | 0.624 | 0 | No change |
| Leaf | Alanine, aspartate, and glutamate metabolism | Fumarate | 0.103 | 0.006 | Increased |
| | | Alanine | <0.001 | 0 | Increased |
| | | Glutamine | 0.728 | 0.178 | No change |
| | | Glutamate | 0.630 | 0.329 | No change |
| | | GABA | 0.674 | 0 | No change |
| Stem | Alanine, aspartate, and glutamate metabolism | **Glutamine** | <0.001 | 0.178 | Decreased |
| | | Alanine | <0.001 | 0 | Increased |
| | | Glutamate | 0.157 | 0.329 | No change |
| | Beta-alanine metabolism | **Beta-alanine** | 0.003 | 0.435 | Decreased |
| | Pantothenate and CoA biosynthesis | **Beta-alanine** | 0.004 | 0.162 | Decreased |
| | | Valine | 0.002 | 0 | Decreased |
| | Arginine and proline metabolism | Glutamine | <0.001 | 0 | Decreased |
| | | Glutamate | 0.157 | 0.127 | No change |

*Note*. GABA: gamma-Aminobutyric acid; HNT: high night-time temperature.

lower grain weight in wheat (Bergkamp, Impa, Asebedo, Fritz, & Jagadish, 2018; Plaut, Butow, Blumenthal, & Wrigley, 2004). Similarly, HNT exposure led to early senescence and a shortened effective grain-filling period (Figure 1), which would hinder the translocation of assimilates to developing grains, resulting in lower kernel weight (Table 1; Garcia et al., 2016). A significant negative effect of HNT on biomass in most of the genotypes (Table 1) would have further resulted in source limitation leading to reduced availability of assimilates to support grain filling (Fischer & Maurer, 1976). Early reproductive organ development in later tillers coinciding with HNT exposure resulted in a lower number of productive spikes, thereby reducing the grain number per plant (Table 1, Supplementary Table S5). This phenomenon is also documented under high-day temperature stress in winter wheat, wherein the sensitive gametogenesis or pollen development are affected in later developing spikes (Bergkamp et al., 2018; Sun et al., 2017). Similarly, a 4°C increase in night-time temperature over ambient, during flowering in field grown wheat, resulted in 6% reduction in grain number per unit area, which was mainly due to a lower number of productive spikes per $m^2$ (Garcia et al., 2015). Hence, lower grain number due to lesser productive spikes and reduced grain weight due to shorter grain-filling duration are the key determinants of HNT-induced yield losses in winter wheat.

## 4.2 | HNT-induced changes in carbon balance and its impact on yield (Objective 2)

A higher rate of reduction in photosynthesis indicated the negative impact of HNT on the photosynthetic machinery. Contrary to photosynthesis, an increase in night respiration indicates significantly higher carbon loss to maintain metabolic functions upon HNT exposure (Figures 3 and 4). A similar phenomenon has been documented in rice exposed to HNT under field conditions (Bahuguna et al., 2017). Night respiration is known to increase exponentially with temperature (Penning de Vries, Witlage, & Kremer, 1979). A 3°C and 6°C increase in night-time temperatures for 2 hr during flowering in cotton resulted in 49% and 56% increase in night respiration, respectively, accompanied with a significant reduction in Adenosine-5′-triphosphate (Loka & Oosterhuis, 2010). It was interesting that four of the six tested genotypes recorded a significant increase in night respiration after 4 days of HNT stress exposure, with all the cultivars regulating carbon loss and demonstrating a different degree of acclimation to extended HNT exposure. This is in line with the hypothesis that night respiration may vary with short- and long-term HNT because of differential response or acclimation of night respiration based on the duration of exposure (Atkin & Tjoelker, 2003; Smith & Dukes, 2013). In addition, it is important to note that the effect of HNT on flag leaf night

respiration was able to provide an overview of the leaf-level changes in carbon dynamics but was unable to capture the severe impact of HNT on the whole plant, including yield traits (Figure 1b; Table 1). Flag leaf night respiration, though non-significant, recorded a negative relationship with grain yield, grain number and thousand grain weight under both control and HNT treatments (Supplementary Figure S2A, B & C). However, days to physiological maturity recorded a positive and negative relationship with flag leaf night respiration under control and HNT treatments, respectively (Supplementary Figure S2D). These results reiterate that, though flag leaf night respiration increases upon HNT, its not an ideal indicator of HNT-induced night respiration and carbon loss in winter wheat. This further emphasizes the need to determine the carbon balance or mechanistic changes under HNT at the whole plant level or by comparing different plant tissues. Overall, the study revealed an increase in night respiration in flag leaves upon exposure to HNT, but this increase in flag leaf night respiration alone was unable to account for HNT-induced changes in yield.

## 4.3 | Metabolic responses on exposure to HNT (Objective 3)

### 4.3.1 | HNT-induced changes in carbohydrate metabolism in spikes

Significant changes in spike metabolites during grain filling would directly impact grain development and weight. Postanthesis HNT stress induced significantly higher metabolic changes in the spike followed by leaf, with stem metabolites being least affected (Supplementary Table S6). An increase in the accumulation of proteinogenic amino acids like glycine, methionine, and alanine under HNT (Table 2; Figure 5) indicates stress-induced protein breakdown or stress adaptive process of amino-acid production (Krasensky & Jonak, 2012; Obata & Fernie, 2012). Proteomic analysis of wheat grains exposed to high day temperature stress revealed starch and sucrose metabolism as one of the major pathways affected under heat stress (Zhang, Pan, et al., 2017). Higher levels of soluble sugars under HNT indicate increased starch breakdown to meet the increased respiratory demand, whereas some sugars like raffinose and maltose are considered as key osmoprotectants that are accumulated under various environmental stresses (Figure 5a, Table 2; Kaplan et al., 2004; Michaletti et al., 2018; Rizhsky et al., 2004). Upon exposure to stress, the simple sugars act as osmolytes maintaining cell turgor, stabilizing cell membranes, and preventing protein degradation (Arbona, Manzi, Ollas, & Gomez-Cadenas, 2013). Moreover, stress-induced accumulation of oligosaccharides such as raffinose and stachyose has been associated with reduced oxidative membrane damage and increased reactive oxygen species scavenging (Molinari et al., 2004). Similar to our findings, HNT-tolerant rice cultivars accumulated higher levels of sugars including glucose, fructose, and sugar alcohols like myo-inositol under HNT compared with control (Figure 6; Glaubitz et al., 2015). Myo-inositol is involved in storage of phosphate in seeds (Loewus & Murthy, 2000). Higher myo-inositol in Tascosa under HNT resulted in increased phosphate in spikes, which is a vital plant nutrient that helps retain better viability to support germination, seedling emergence, and early growth (Figure 6; Loewus & Murthy, 2000). A greater assimilate contribution through awns and spike photosynthesis under stress has been reported in wheat (Maydup et al., 2010; Toriba & Hirano, 2014), indicating the importance of maintaining spike photosynthetic capacity under postheading HNT exposure. In our study, spike metabolite analysis was carried out from two to 12 DAH, when the floral tissue is actively involved in carbon assimilation (Sanchez-Bragado, Molero, Reynolds, & Araus, 2014). Hence, HNT-induced accumulation of maltose in spikes of Tascosa (Figure 7) could contribute towards protecting the photosynthetic electron transport chain, proteins, and membranes in chloroplast stroma, enhancing its tolerance to HNT (Kaplan & Guy, 2004). Induction of beta-amylase and subsequent maltose accumulation aided *Arabidopsis* knockout mutants to cope with acute heat and cold shock and has been indicated that this could well continue to operate under long-term stress exposure (Kaplan & Guy, 2004). Moreover, maltose production is straightforward involving a single step reaction, and hence, plants with adequate starch content can produce significant amounts of maltose in very short time-frame, unlike other protectants (Kaplan & Guy, 2004). Higher levels of sucrose and maltose in C3 grass species under elevated $CO_2$ played a crucial role in mitigating heat stress (Yu, Du, Xu, & Huang, 2012). Reduced photosynthetic efficiency of source tissue under abiotic stresses alters carbon balance, further limiting the supply of soluble sugars to sink (Lemoine et al., 2013). A similar response leading to lower sugar levels in the spikes of the sensitive genotype (TX86A5606) was recorded under HNT (Figure 6).

### 4.3.2 | HNT-induced activation of TCA cycle and amino acid metabolism in leaf

Unlike in spike, leaf glycine was significantly reduced under HNT, especially in the susceptible genotype TX86A5606, which indicates dehydration of serine in the presence of serine dehydratase to form pyruvate, the principal substrate of TCA cycle to meet the high respiration demand under HNT (Hildebrandt, Nesi, Araujo, & Braun, 2015). Moreover, a significant increase in intermediates of TCA cycle compounds like isocitrate and fumarate were recorded in rice leaves exposed to HNT, likely reflecting an increase in respiration (Figure 5 b; Glaubitz et al., 2017). These significant alterations in leaf metabolites supports a severe negative impact of HNT-induced higher night respiration at the whole plant level, thereby reducing the overall biomass, compared with the acclimative response recorded by flag leaf night respiration in our study (Table 1). Leaves of TX86A5606 exposed to HNT resulted in an increased accumulation of tyrosine an aromatic amino acid in plants produced through shikimate pathway (Figure 6b). Shikimate pathway is known to be up-regulated under water-limited conditions, especially in drought-sensitive wheat genotype (Michaletti et al., 2018). In Tascosa leaves, aspartate-derived amino acids like lysine and leucine were reduced and methionine was increased under HNT, possibly regulating the hormonal balance needed to minimize the HNT damage but such dynamic changes were not noticed in TX86A5606. Phytohormones like abscisic acid (ABA) and ethylene are known to increase under heat stress whereas others such as cytokinin, auxin, and gibberellic acid decreased in response to heat stress (Bita & Gerats, 2013). Heat stress-induced early maturity could well be related to increased accumulation of ABA and ethylene and

reduced levels of auxins (Binder & Patterson, 2009). An increase in methionine (possibly due to the conversion of S-Adenosyl methionine back to methionine), indicates a lower ethylene production, potentially countering HNT-induced early senescence in Tascosa. Stem metabolites were least affected and most of the affected amino acids recorded a reduction under HNT, which could be due to a lower production and transport by leaves or higher demand by sink (Figure 5c). Overall, the study has identified significant increases in sugars, like glucose, fructose, and maltose, sugar alcohols like myo-inositol in spikes of HNT-tolerant (Tascosa) and TCA cycle intermediate compounds like fumarate and isocitrate in leaves of HNT-sensitive genotype (TX86A5606).

The metabolites with significant alterations under HNT, especially in the tolerant genotype, could be used to develop metabolite-based markers to support wheat breeding programmes focused on improving abiotic stress tolerance. The candidate metabolites identified in this study including soluble sugars and TCA cycle intermediates after validating under field conditions, could be used as target proxies to screen diverse germplasm or mapping populations to identify genomic regions (Zhang, Saito, & Sharma, 2017) controlling these metabolites. An alternative option would be to identify the rate-limiting step/enzyme in the metabolite pathway, which is most responsive to HNT and develop gene-based markers targeting specific enzyme/s. These metabolite or gene-based DNA markers can be directly used for selecting HNT tolerant lines during breeding cycles.

In conclusion, winter wheat genotypes exhibited considerable variation in HNT-induced increase in flag leaf night respiration and acclimation upon extended HNT exposure. A greater reduction in biomass, yield, and yield-related traits under HNT compared with changes in flag leaf carbon balance cautions the need to consider carbon balance at whole plant level. Alterations in carbohydrate metabolism in spikes and TCA cycle in leaves provides novel insights into metabolites involved in HNT response. Our findings contribute towards understanding the mechanistic responses to HNT and help in developing markers to support ongoing breeding programmes aimed at enhancing heat stress resilience in wheat.

## ACKNOWLEDGEMENTS

We thank the financial support by National Science Foundation, USA Award No. 1736192 to Krishna Jagadish, Kansas State University and Toshihiro Obata at University of Nebraska, Lincoln. Contribution 19-029-J from the Kansas Agricultural Experiment Station.

## AUTHOR CONTRIBUTIONS

S. M. I., S. V. K. J. designed the experiment; S. M. I. conducted the experiments; S. M. I. and J. S. V. S. recorded the photosynthesis and respiration data; I. K. and T. O. generated metabolomics data; S. M. I. and T. O. analyzed the metabolomics data; S. M. I., R. B., S. V. K. J., and T. O. organized, analyzed, and interpreted the data; and S. M. I., R. B., T. O., and S. V. K. J. drafted and edited the manuscript.

## ORCID

*S.V. Krishna Jagadish* https://orcid.org/0000-0002-1501-0960

## REFERENCES

Alexander, L. V., Zhang, X., Peterson, T. C., Caesar, J., Gleason, B., Tank, A. M. G. K., … Vazquez-Aguirre, J. L. (2006). Global observed changes in daily climate extremes of temperature and precipitation. *Journal of Geophysical Research-Atmospheres*, *111*, D05109.

Arbona, V., Manzi, M., Ollas, C., & Gomez-Cadenas, A. (2013). Metabolomics as a tool to investigate abiotic stress tolerance in plants. *International Hournal of Molecular Sciences*, *14*, 4885–4911. https://doi.org/10.3390/ijms14034885

Asseng, S., Ewert, F., Martre, P., Rotter, R. P., Lobell, D. B., Cammarano, D., … Zhu, Y. (2015). Rising temperatures reduce global wheat production. *Nature Climate Change*, *5*, 143–147. https://doi.org/10.1038/nclimate2470

Atkin, O. K., Bruhn, D., Hurry, V. M., & Tjoelker, M. G. (2005). Evans Review No. 2: The hot and the cold: Unravelling the variable response of plant respiration to temperature. *Functional Plant Biology*, *32*, 87–105. https://doi.org/10.1071/FP03176

Atkin, O. K., Scheurwater, I., & Pons, T. L. (2007). Respiration as a percentage of daily photosynthesis in whole plants is homeostatic at moderate, but not high, growth temperatures. *New Phytologist*, *174*, 367–380. https://doi.org/10.1111/j.1469-8137.2007.02011.x

Atkin, O. K., & Tjoelker, M. G. (2003). Thermal acclimation and the dynamic response of plant respiration to temperature. *Trends in Plant Science*, *8*, 343–351. https://doi.org/10.1016/S1360-1385(03)00136-5

Bahuguna, R., Solis, C., Shi, W., & Jagadish, S. V. K. (2017). Post-flowering night respiration and altered sink activity account for high night temperature-induced grain yield and quality loss in rice (*Oryza sativa* L.). *Physiologia Plantarum*, *159*, 59–73. https://doi.org/10.1111/ppl.12485

Bergkamp, B., Impa, S. M., Asebedo, A. R., Fritz, A. K., & Jagadish, S. V. K. (2018). Prominent winter wheat varieties response to post-flowering heat stress under controlled chambers and field based heat tents. *Field Crops Research*, *222*, 143–152. https://doi.org/10.1016/j.fcr.2018.03.009

Binder, B. M., & Patterson, S. E. (2009). Ethylene-dependent and -independent regulation of abscission. *Stewart Postharvest Review*, *5*, 1–10.

Bita, C. E., & Gerats, T. (2013). Plant tolerance to high temperature in a changing environment: Scientific fundamentals and production of heat stress-tolerant crops. *Frontiers in Plant Science*, *273*, 1–18.

Calderini, D. F., Savin, R., Abeledo, L. G., Reynolds, M. P., & Slafer, G. A. (2001). The importance of the period immediately preceding anthesis for grain weight determination in wheat. *Euphytica*, *119*, 199–204. https://doi.org/10.1023/A:1017597923568

Dai, A., Wigley, T. M. L., Boville, B. A., Kiehl, J. T., & Buja, L. E. (2001). Climates of the twentieth and twenty-first centuries simulated by the NCAR climate system model. *Journal of Climate*, *14*, 485–519. https://doi.org/10.1175/1520-0442(2001)014<0485:COTTAT>2.0.CO;2

Easterling, D. R., Horton, B., Jones, P. D., Peterson, T. C., Karl, T. R., Parker, D. E., … Folland, C. K. (1997). Maximum and minimum temperature trends for the globe. *Science*, *277*, 364–367. https://doi.org/10.1126/science.277.5324.364

Ehtaiwesh, A. F. A. (2016). Effects of salinity and high temperature stress on winter wheat genotypes. Thesis dissertation submitted to Kansas state university, USA. http://hdl.handle.net/2097/34545.

Fernandez-Long, M. E., Muller, G. V., Beltran-Przekurat, A., & Scarpati, O. E. (2013). Long-term and recent changes in temperature-based agroclimatic indices in Argentina. *International Journal of Climatology*, *33*, 1673–1686. https://doi.org/10.1002/joc.3541

Fernie, A. R., Aharoni, A., Willmitzer, L., Stitt, M., Tohge, T., Kopka, J., … DeLuca, V. (2011). Recommendations for reporting metabolite data. *Plant Cell*, *23*, 2477–2482. https://doi.org/10.1105/tpc.111.086272

Fischer, R. A., & Maurer, O. R. (1976). Crop temperature modification and yield potential in a dwarf spring wheat. *Crop Science*, *16*(6), 855–859. https://doi.org/10.2135/cropsci1976.0011183X001600060031x

Garcia, G. A., Dreccer, M. F., Miralles, D. J., & Serrago, R. A. (2015). High night temperatures during grain number determination reduce wheat and barley grain yield: A field study. *Global Change Biology*, *21*, 4153–4164. https://doi.org/10.1111/gcb.13009

Garcia, G. A., Serrago, R. A., Dreccer, M. F., & Miralles, D. J. (2016). Post-anthesis warm nights reduce grain weight in field-grown wheat and barley. *Field Crops Research*, *195*, 50–59. https://doi.org/10.1016/j.fcr.2016.06.002

Glaubitz, U., Erban, A., Kopka, J., Hincha, D. K., & Zuther, E. (2015). High night temperature strongly impacts TCA cycle, amino acid and ploy amine biosynthetic pathways in rice in a sensitivity-dependent manner. *Journal of Experimental Botany*, *66*, 6385–6397. https://doi.org/10.1093/jxb/erv352

Glaubitz, U., Li, X., Schaedel, S., Erban, A., Sulpice, R., Kopka, J., … Zuther, E. (2017). Integrated analysis of rice transcriptomic and metabolomics responses to elevated night temperatures indetifies sensitivity and tolerance-related profiles. *Plant, Cell & Environment*, *40*, 121–137. https://doi.org/10.1111/pce.12850

Hildebrandt, T. M., Nesi, A. N., Araujo, W. L., & Braun, H. P. (2015). Amino acid catabolism in plants. *Molecular Plant*, *8*, 1563–1579. https://doi.org/10.1016/j.molp.2015.09.005

IPCC (2014). Climate change 2014: synthesis report. In Core Writing Team, R. K. Pachauri, & L. A. Meyer (Eds.), *Contribution of working groups I, II and III to the Fifth Assessment report of the Intergovernmental Panel on Climate Change*. Geneva, Switzerland: IPCC.

Jagadish, S. V. K., Murty, M. V. R., & Quick, W. P. (2015). Rice responses to raising temperatures – challenges, perspectives and future directions. *Plant, Cell and Environment*, *38*, 1686–1698. https://doi.org/10.1111/pce.12430

Kaplan, F., & Guy, C. L. (2004). Beta-Amylase induction and the protective role of maltose during temperature shock. *Plant Physiology*, *135*, 1674–1684. https://doi.org/10.1104/pp.104.040808

Kaplan, F., Kopka, J., Haskell, D. W., Zhao, W., Schiller, C., Gatzke, N., … Guy, C. L. (2004). Exploring the temperature-stress metabolome of Arbidopsis. *Plant Physiology*, *136*, 4159–4168. https://doi.org/10.1104/pp.104.052142

Kopka, J., Schauer, N., Krueger, S., Birkemeyer, C., Usadel, B., Bergmüller, E., … Steinhauser, D. (2005). GMD@CSB.DB: the Golm metabolome database. *Bioinformatics*, *21*, 1635–1638. https://doi.org/10.1093/bioinformatics/bti236

Krasensky, J., & Jonak, C. (2012). Drought, salt, and temperature stress-induced metabolic rearrangements and regulatory networks. *Journal of Experimental Botany*, *63*, 1593–1608. https://doi.org/10.1093/jxb/err460

Lemoine, R., Camera, S. L., Atanassova, R., Dedaldechamp, F., Allario, T., Pourtau, N., … Durand, M. (2013). Source-to-sink transport of sugar and regulation by environmental factors. *Frontiers in Plant Science*, *4*(272). http://doi.org/10.3389/fpls.2013.00272

Li, X., Lawas, L. M. F., Malo, R., Glaubitz, U., Erban, A., Mauleon, R., … Jagadish, S. V. K. (2015). Metabolic and transcriptomic signatures of rice floral organs reveal sugar starvation as a factor in reproductive failure under heat and drought stress. *Plant, Cell and Environment*, *30*(10), 2171–2192.

Liang, J., Xia, J., Liu, L., & Wan, S. (2013). Global patterns of the responses of leaf-level photosynthesis and respiration in terrestrial plants to experimental warming. *Journal of Plant Ecology*, *6*, 437–447. https://doi.org/10.1093/jpe/rtt003

Lisec, J., Schauer, N., Kopka, J., Willmitzer, L., & Fernie, A. R. (2006). Gas chromatography mass spectrometry-based metabolite profiling in plants. *Nature Protocols*, *1*, 387–396. https://doi.org/10.1038/nprot.2006.59

Lobell, D. B., Sibley, A., & Ortiz-Monasterio, J. I. (2012). Extreme heat effects on wheat senescence in India. *Nature Climate Change*, *2*, 186–189. https://doi.org/10.1038/nclimate1356

Loewus, F. A., & Murthy, P. P. N. (2000). Myo-Inositol metabolism in plants. *Plant Science*, *150*, 1–19. https://doi.org/10.1016/S0168-9452(99)00150-8

Loka, D. A., & Oosterhuis, D. M. (2010). Effect of high night temperature on cotton respiration, ATP levels and carbohydrate content. *Environmental and Experimental Botany*, *68*, 258–263. https://doi.org/10.1016/j.envexpbot.2010.01.006

Luedemann, A., von Malotky, L., Erban, A., & Kopka, J. (2012). TagFinder: Preprocessing software for the fingerprinting and the profiling of gas chromatography-mass spectrometry based metabolome analyses. *Methods in Molecular Biology*, *860*, 255–286. https://doi.org/10.1007/978-1-61779-594-7_16

Maydup, M. L., Antonietta, M., Guiamett, J. J., Graciano, C., Lopez, J. R., & Tambussi, E. A. (2010). The contribution of ear photosynthesis to grain filling in bread wheat (*Triticum aestivum* L.). *Field Crops Research*, *119*, 48–58. https://doi.org/10.1016/j.fcr.2010.06.014

Michaletti, A., Naghavi, M. R., Toorchi, M., Zolla, L., & Rinalducci, S. (2018). Metabolomics and proteomics drought-stress responses of leaf tissues from spring-wheat. *Scientific Reports*, *8*, 5710. https://doi.org/10.1038/s41598-018-24012-y

Molinari, H. B. C., Marur, C. J., Filho, J. C. B., Kobayashi, A. K., Pileggi, M., Junior, R. P. l., … Vieira, L. G. E. (2004). Osmotoic adjustment in transgenic citrus rootstock Carrizo citrange (Citrus sinensis Osb. x *Poncirus trifoliate* L. Raf.) overproducing proline. *Plant Science*, *167*, 1357–1381.

Narayanan, S., Prasad, P. V. V., Fritz, A. K., Boyle, D. L., & Gill, B. S. (2015). Impact of high night-time and high daytime temperature stress on winter wheat. *Journal of Agronomy and Crop Science*, *201*, 206–218. https://doi.org/10.1111/jac.12101

Obata, T., & Fernie, A. R. (2012). The use metabolomics to dissect plant responses to abiotic stresses. *Cellular and Molecular Life Sciences*, *69*, 3225–3243. https://doi.org/10.1007/s00018-012-1091-5

Penning de Vries, F. W. T., Witlage, J. M., & Kremer, D. (1979). Rates of respiration and increase in structural dry matter in young wheat, ryegrass and maize plants in relation to temperature, to water stress and to their sugar content. *Annals of Botany*, *44*, 595–609. https://doi.org/10.1093/oxfordjournals.aob.a085772

Peraudeau, S., Lafarge, T., Roques, S., Quinones, C., Clément-Vidal, A., Ouwerkerk, P., … Dingkuhn, M. (2015). Effects of carbohydrates and night temperature on night respiration in rice. *Journal of Experimental Botany*, *66*(13), 3931–3944. https://doi.org/10.1093/jxb/erv193

Pinto, R. S., Molero, G., & Reynolds, M. P. (2017). Identification of heat tolerant wheat lines showing genetic variation in leaf respiration and other physiological traits. *Euphytica*, *213*, 76. https://doi.org/10.1007/s10681-017-1858-8

Plaut, Z., Butow, B. J., Blumenthal, C. S., & Wrigley, C. W. (2004). Transport of dry matter into developing wheat kernels and its contribution to grain yield under post anthesis water deficit and elevated temperature. *Field Crops Research*, *86*, 185–198. https://doi.org/10.1016/j.fcr.2003.08.005

Prasad, P. V. V., Bheemanahalli, R., & Jagadish, S. V. K. (2017). Field crops and the fear of heat stress—opportunities, challenges and future directions. *Field Crops Research*, *200*, 114–121. https://doi.org/10.1016/j.fcr.2016.09.024

Rizhsky, l., Liang, H., Shuman, J., Shulaev, V., Davletova, S., & Mittler, R. (2004). When defense pathways collide. The response of Arabidopsis to a combination of drought and heat stress. *Plant Physiology*, *134*, 1683–1696. https://doi.org/10.1104/pp.103.033431

Sakuraba, Y., Lee, S. H., Kim, Y. S., Park, O. K., Hortensteiner, S., & Paek, N. C. (2014). Delayed degradation of chlorophylls and photosynthetic proteins in Arabidopsis autophagy mutants during stress-induced leaf yellowing. *Journal of Experimental Botany*, *65*, 3915–3925. https://doi.org/10.1093/jxb/eru008

Sanchez-Bragado, R., Molero, G., Reynolds, M. P., & Araus, J. L. (2014). Relative contribution of shoot and ear photosynthesis to grain filling in wheat under good agronomic conditions assessed by differential organ

$\delta^{13}C$. *Journal of Experimental Botany*, *65*, 5401–5413. https://doi.org/10.1093/jxb/eru298

Shi, W., Muthurajan, R., Rahman, H., Selvam, J., Peng, S., Zou, Y., & Jagadish, S. V. K. (2013). Source-sink dynamics and proteomic reprogramming under elevated night temperature and their impact on rice yield and grain quality. *New Phytologist*, *197*, 825–837. https://doi.org/10.1111/nph.12088

Shi, W., Yin, X., Struik, P. C., Xie, F., Schmidt, R. C., & Jagadish, S. V. K. (2016). Grain yield and quality responses of tropical hybrid rice to high night-time temperature. *Field Crops Research*, *190*, 18–25. https://doi.org/10.1016/j.fcr.2015.10.006

Shulaev, V., Cortes, D., Miller, G., & Mittler, R. (2008). Metabolomics for plant stress response. *Physiologia Plantarum*, *132*, 199–208. https://doi.org/10.1111/j.1399-3054.2007.01025.x

Sillmann, J., Kharin, V. V., Zhang, X., Zwiers, F. W., & Bronaugh, D. (2013). Climate extremes indices in the CMIP5 multi-model ensemble: Part 1. Model evaluation in the present climate. *Journal of Geophysical Research-Atmospheres*, *118*, 1716–1733. https://doi.org/10.1002/jgrd.50203

Sillmann, J., Kharin, V. V., Zwiers, F. W., Zhang, X., & Bronaugh, D. (2013). Climate extremes indices in the CMIP5 multi-model ensemble: Part 2. Future climate projections. *Journal of Geophysical Research-Atmospheres*, *118*, 2473–2493. https://doi.org/10.1002/jgrd.50188

Singh, A., Kumar, P., Sharma, M., Tuli, R., Dhaliwal, H. S., Chaudhury, A., … Roy, J. (2015). Expression patterns of genes involved in starch biosynthesis during seed development in bread wheat (*Triticum aestivum*). *Molecular Breeding*, *35*, 1–9.

Smith, N. G., & Dukes, J. S. (2013). Plant respiration and photosynthesis in global-scale models: Incorporating acclimation to temperature and $CO_2$. *Global Change Biology*, *19*, 45–63. https://doi.org/10.1111/j.1365-2486.2012.02797.x

Sun, A., Impa, S. M., Sunoj, V. S. J., Singh, K., Gill, K. S., Prasad, P. V. V., & Jagadish, S. V. K. (2017). Heat stress during flowering affects time of day of flowering, seed-set and grain quality in spring wheat (*Triticum aestivum* L.). *Crop Science*, *58*, 380–392.

Swain, P., Baig, M. J., & Naik, S. K. (2000). Maintenance respiration of *Oryza sativa* leaves at different growth stages as influenced by nitrogen supply. *Biologia Plantarum*, *43*, 587–590. https://doi.org/10.1023/A:1002810923897

Tank, A. M. G. K., Peterson, T. C., Quadir, D. A., Dorji, S., Zou, X., Tang, H., … Spektorman, T. (2006). Changes in daily temperature and precipitation extremes in central and south Asia. *Journal of Geophysical Research*, *111*, D16105. https://doi.org/10.1029/2005JD006316

Toriba, T., & Hirano, H. Y. (2014). The DROOPING LEAF and OsETTIN2 genes promote awn development in rice. *Plant Journal*, *77*, 616–626. https://doi.org/10.1111/tpj.12411

Vincent, L. A., & Mekis, E. (2006). Changes in daily and extreme temperature and precipitation indices for Canada over the twentieth century. *Atmosphere-Ocean*, *44*, 177–193. https://doi.org/10.3137/ao.440205

Vose, R. S., Easterling, D. R., & Gleason, B. (2005). Maximum and minimum temperature trends for the globe: An update through 2004. *Geophysical Research Letters*, *32*, L23822. https://doi.org/10.1029/2005GL024379

Xia, J., & Wishart, D. S. (2010). MetPA: A web-based metabolomics tool for pathway analysis and visualization. *Bioinformatics*, *26*(18), 2342–2344. https://doi.org/10.1093/bioinformatics/btq418

Yu, J., Du, H., Xu, M., & Huang, B. (2012). Metabolic responses to heat stress under elevated atmospheric $CO_2$ concentration in a cool-season grass species. *Journal of the American Society for Horticultural Science*, *137*(4), 221–228.

Zhang, G., Saito, R., & Sharma, K. (2017). A metabolite-GWAS (mGWAS) approach to unveil chronic kidney disease progression. *Kidney International*, *91*(6), 1274–1276. https://doi.org/10.1016/j.kint.2017.03.022

Zhang, Y., Pan, J., Huang, X., Guo, D., Lou, H., Hou, Z., … Li, B. (2017). Differential effects of a post-anthesis heat stress on wheat (*Triticum aestivum* L.) grain proteome determined by iTRAQ. *Scientific Reports*, *7*, 3468. https://doi.org/10.1038/s41598-017-03860-0

## SUPPORTING INFORMATION

Additional supporting information may be found online in the Supporting Information section at the end of the article.

**How to cite this article:** Impa SM, Sunoj VSJ, Krassovskaya I, Bheemanahalli R, Obata T, Jagadish SVK. Carbon balance and source-sink metabolic changes in winter wheat exposed to high night-time temperature. *Plant Cell Environ*. 2019;42:1233–1246. https://doi.org/10.1111/pce.13488